Письма в ЭЧАЯ. 2009. Т. 6, № 3(152). С. 399–406

SIMULATION OF MUON-INDUCED AIR SHOWERS AFFECTING CMS TRACKING DETECTORS

A. Mahrous [a], *M. Sherif* [b], *M. Soliman* [c]

[a] Physics Dept., Faculty of Science, Helwan University, Cairo, Egypt
[b] Physics Dept., Faculty of Science, Cairo University, Cairo, Egypt
[c] High Energy Physics Lab., Faculty of Science, Cairo University, Egypt

We study the propagation of energetic muons produced by ultrahigh energy cosmic rays which could penetrate the cavern of a giant experiment called Compact Muon Solenoid (CMS) at CERN. The present work is based on our previous simulation model proposed in [1]. We have improved this model by (1) eliminating the ambiguity via adding Landau–Pomeranchuk–Migdal effect to the Monte-Carlo code, (2) using different incidence angles of the simulated air showers, (3) defining the actual contents of the CMS cavern concrete. We estimate the energy spectrum of muons produced by air showers of primary protons and photons, which could be detected as a background in the CMS tracking detectors. Our results show that muons produced by air showers within the energy range 10^{17}–10^{20} eV injected to the CMS site could penetrate the cavern with cutoff energy 36.5 GeV.

Мы изучаем распространение энергетичных мюонов, рожденных в космических лучах сверхвысоких энергий, которые могут проникать в шахту, где размещен масштабный эксперимент «Компактный мюонный соленоид» (CMS) (ЦЕРН). Настоящая работа основана на моделировании, предложенном нами ранее в [1]. Модификация состоит: 1) в устранении неопределенности с помощью учета в монте-карловской программе эффекта Ландау–Померанчука–Мигдала, 2) в использовании различных углов падения в моделируемых атмосферных ливнях, 3) в определении фактического состава бетона в шахте CMS. Мы оцениваем энергетический спектр мюонов, рожденных атмосферными ливнями первичных протонов и фотонов, которые могли бы быть зарегистрированы как фон в трековых детекторах CMS. Наши результаты указывают на то, что мюоны, рожденные атмосферными ливнями в энергетическом интервале 10^{17}–10^{20} эВ и достигшие местоположения CMS, могут проникать в шахту, если их энергия больше 36,5 ГэВ.

PACS: 96.50.Sd; 29.40.Gx; 95.55.Vj

INTRODUCTION

The initial discovery of the muon was not received very well, because it shattered many theories of matter and energy. Today, the muon is an integral part of almost every field of physics including elementary particles theories, chemistry and nuclear structure [2]. At the time, this newly discovered particle was thought to be a meson, a bound state of two quarks, predicted by Yukawa. The particle he predicted was the carrier of the nuclear force, its mass ($\approx$ 207 MeV) was close to the predicted value of the Yukawa's particle. However, this «mu-meson», as it was called later, was found to be a deeply penetrating particle as it was detected in deep underground mines. Evidently, if the particle was to travel through thousands of feet of matter, it did not interact strongly with matter, as the carrier of the nuclear force should.

The interaction of cosmic ray particles in the upper atmosphere (primarily 9–15 km above Earth's surface) usually produces pions [3], a bound state of an up and anti-down quark. With lifetime of ($2.6 \cdot 10^{-8}$ s), the pion travels only hundreds of meters at velocities between (0.966 c and 0.977 c) before decaying into a muon and mu-neutrino $\pi^{\pm} \rightarrow \mu^{\pm} + \nu_{\mu}$. The muons produced in that reaction descend to Earth's surface with ample supply of muons at sea level which facilitates the study of these particles [4]. An accurate simulation of the propagation of muons through matter is needed for the analysis of data produced by muons in underground experiments. As muon travels through matter, it looses energy due to ionization losses, bremsstrahlung, photonuclear interaction and pair production [5]. All of these losses have continuous and stochastic components got from Bethe–Bloch restricted energy loss formula. That formula was modified for muon charged leptons following the procedure outlined in [6] and [7], and can be written as follows:

$$\left[\frac{dE}{dx}\right]_{T\langle T_{\rm cut}\rangle} = 2\pi r_e^2 mc^2 n_{\rm el} \frac{(Z_p)^2}{\beta^2}\left[\ln\left(\frac{2mc^2\beta^2\gamma^2 T_{\rm up}}{I^2}\right) - \beta^2\left(1+\frac{T_{\rm up}}{T_{\rm max}}\right) - \delta - \frac{2C_e}{Z}\right]. \tag{1}$$

Knowing that maximum energy transfer in a single collision is given by

$$T_{\rm max} = \frac{2mc^2(\gamma^2-1)}{1+2\gamma(m/M)+(m/M)^2}, \tag{2}$$

where m — electron mass; M — muon mass; r_e — classical electro radius $e^2/(4\pi\varepsilon_{\rm o}mc^2)$; mc^2 — mass-energy of the electron; $n_{\rm el}$ — electron density in the material; I — mean excitation energy; γ — E/mc^2; β^2 — $1-(1/\gamma^2)$; $T_{\rm up}$ — min ($T_{\rm cut}$, $T_{\rm max}$); δ — density effect function; C_e — shell correction function.

Surface muon observations have significant responses from approximately 10 GeV to several hundreds GeV, while underground muon observations extend up to slightly above 1000 GeV, the latter can penetrate long depths under the ground.

Imagining how much the energy of the energetic cosmic ray is, the Large Hadronic Collider (LHC) at CERN is built to accelerate protons to energies up to $7{\cdot}10^{12}$ eV in the 27 km tunnel beneath the French/Swiss border. We have measured cosmic ray particles with energies almost 8 orders of magnitude above this. Currently, the energy record is held by a particle observed by the fly's eye experiment which carried an energy of $3.2 \cdot 10^{20}$ eV [8]. Our paper studies the penetration of the muons produced by such energetic air showers to the CMS cavern at CERN, which could be detected as a background in the tracking detectors.

1. THE LPM EFFECT

The Landau–Pomeranchuk–Migdal (LPM) effect results in the suppression of the Bethe–Heitler cross section for the highest energy component of showers and the subsequent significant elongation of the extensive air showers [9]. Its threshold depends on the ratio of the energy of the primary particle to the density of the interaction medium. Multiple scattering changes the muon trajectory within the interaction distance, therefore, it suppresses the bremsstrahlung [10]. At high enough energies, the LPM effect increases the effective radiation length, which lengthens electromagnetic showers. At first we remind here the semiclassical

picture of the LPM effect when the muon is of a sufficiently high momentum. The longitudinal momentum carried by the virtual photon equals

$$q = p_\mu - p_\mu{}' - \kappa = \sqrt{E_\mu^2 - m_\mu^2} - \sqrt{E_\mu'^2 - m_\mu^2} - E_\gamma, \tag{3}$$

where P_μ, P'_μ, E_μ and E'_μ are the muon momentum and energy before and after the interaction, respectively; E_γ is the photon energy and γ is Lorentz factor. For high energy muons this simplifies to

$$q = \frac{m_\mu^2 E_\gamma}{2E_\mu\,(E_\mu - E_\gamma)} = \frac{m_\mu}{2\gamma}\,\frac{u}{1-u}, \tag{4}$$

where $u = E_\gamma / E_\mu$ is the fractional energy of the radiated photon. In our simulation, we took the LPM effect into account considering that the muon must be undisturbed while it traverses to the CMS cavern.

2. THE CMS CAVERN

The gigantic cavern for the CMS is designed to protect the detectors from background radiation; it is located near the village of Cessy in France at 100 m underground. The cavern is 53 m long, 27 m wide and 24 m in height. The design and construction of the cavern is shown in Fig. 1. There are three layers sited above the CMS detectors. The first layer is molasses of 30 m thickness followed by a layer of 30 m thickness of concrete and 40 m of air. The thickness and material of each layer have been adapted in the simulation of the penetrating underground muons.

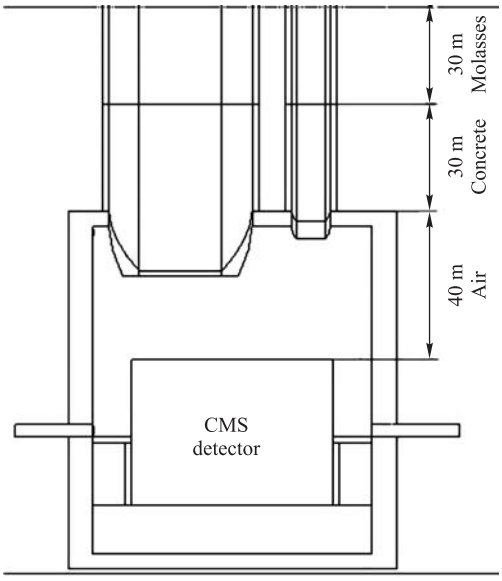

Fig. 1. Design and construction of the CMS cavern

3. SIMULATION RESULTS

Our simulation is divided into two parts, the first part including the simulation of the interaction of primary cosmic ray protons and photons with the atmosphere to estimate the energy spectrum of muons reaching the ground level. This is the input to the second part — Monte-Carlo simulation — to calculate the muons spectrum penetrating the CMS cavern.

The energy spectrum of muons reaching the ground level produced by primary protons is shown in logarithmic scale in Fig. 2. The four curves in the figure are corresponding to primary energies, from down to up, 10^{17}, 10^{18}, 10^{19} and 10^{20} eV, respectively. We used the QGSJET model in Aires V.2.2.4 (http://www.fisica.unlp.edu.ar/auger/aires/) to produce such

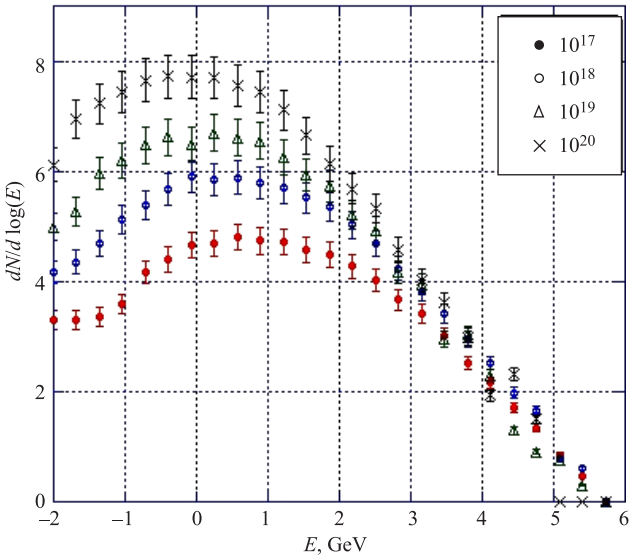

Fig. 2. The energy spectrum (in logarithmic scale) of muons reaching the ground level produced by primary protons. The four curves are corresponding to primary energies, from down to up, 10^{17}, 10^{18}, 10^{19} and 10^{20} eV, respectively

air showers after setting the geomagnetic conditions at the CMS location. The figure shows that muons arrive at the ground level within the energy range from 0.01 GeV to $3.2 \cdot 10^5$ GeV. In this case, the four curves are coincident in the higher part of the muons spectrum with energy greater than 100 GeV.

The energy spectrum of muons reaching the ground level produced by primary photons is shown in logarithmic scale in Fig. 3. The four curves in the figure are corresponding to primary energies, from down to up, 10^{17}, 10^{18}, 10^{19} and 10^{20} eV, respectively. The figure shows that muons reach the ground level within the energy range from 0.03 GeV to $3.2 \cdot 10^4$ GeV, moreover, the four curves are coincident in the higher part of the muons spectrum with energy greater than 300 GeV.

The lateral distribution of muons produced by primary protons and photons is shown in Figs. 4 and 5, respectively. The four curves in each figure are corresponding to primary energies, from down to up, 10^{17}, 10^{18}, 10^{19} and 10^{20} eV, respectively. The two figures show

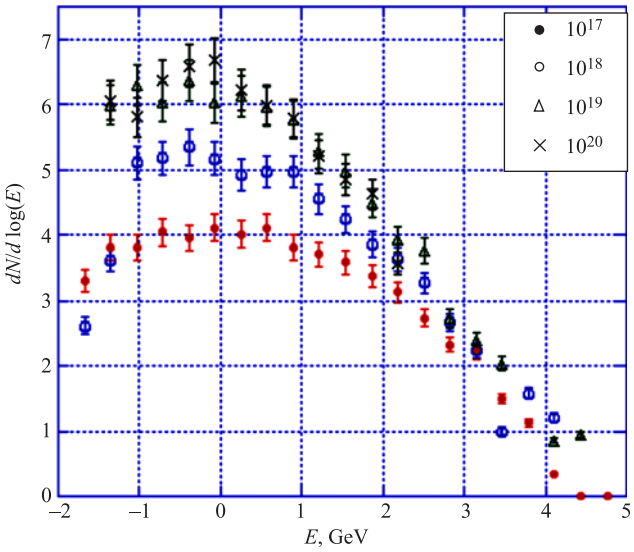

Fig. 3. The energy spectrum (in logarithmic scale) of muons reaching the ground level produced by primary photons. The four curves are corresponding to primary energies, from down to up, 10^{17}, 10^{18}, 10^{19} and 10^{20} eV, respectively

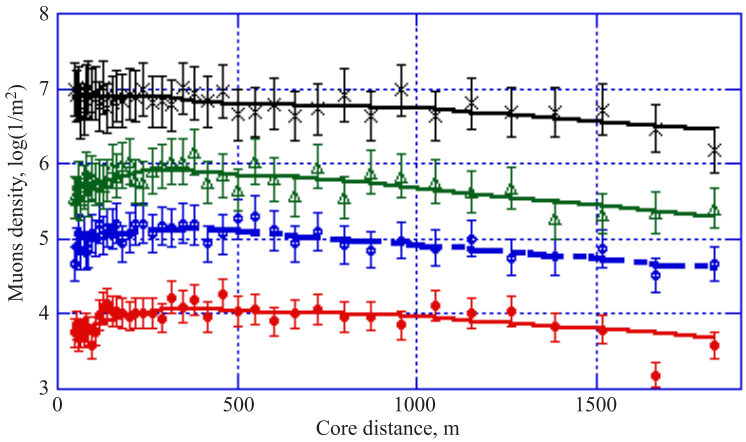

Fig. 4. The lateral distribution of muons density measured from the shower core. The four curves are corresponding to primary proton energies, from down to up, 10^{17}, 10^{18}, 10^{19} and 10^{20} eV, respectively

that muon component of the shower width is covering a circular area of radius 1.8 km from the shower core; in addition, the muon density produced by primary protons is ten times larger than that produced by primary photons.

The energy spectrum of muons penetrating the CMS cavern produced by primary protons is shown in logarithmic scale in Fig. 6. The four curves in the figure are corresponding to primary energies, from down to up, 10^{17}, 10^{18}, 10^{19} and 10^{20} eV, respectively. The cutoff

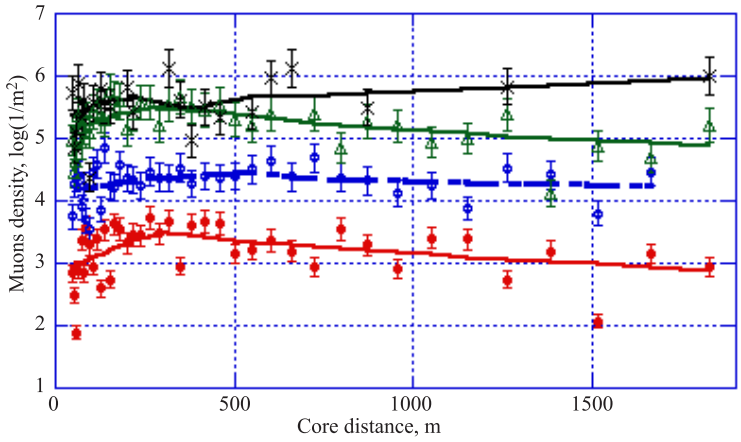

Fig. 5. The lateral distribution of muons density measured from the shower core. The four curves are corresponding to primary photon energies, from down to up, 10^{17}, 10^{18}, 10^{19} and 10^{20} eV, respectively

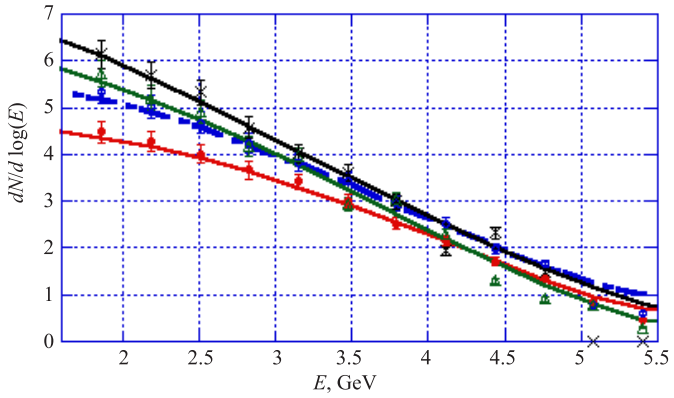

Fig. 6. The energy spectrum (in logarithmic scale) of muons penetrating the CMS cavern produced by primary protons. The four curves are corresponding to primary energies, from down to up, 10^{17}, 10^{18}, 10^{19} and 10^{20} eV, respectively

energy of the spectrum curves occurs at muon energy $E_{\text{cut}} = 36.5$ GeV, which means that muons with higher energy could penetrate the CMS cavern.

The energy spectrum of muons penetrating the CMS cavern produced by primary photons is shown in logarithmic scale in Fig. 7. The four curves in the figure are corresponding to primary energies, from down to up, 10^{17}, 10^{18}, 10^{19} and 10^{20} eV, respectively. The cutoff energy is almost the same as in the previous case of primary protons, which occurred at $E_{\text{cut}} = 36.5$ GeV. The relationship between the energy of primary incident muons at ground level E_{in} and energy of transmitted muons to the CMS detectors E_{tr} is shown in Fig. 8. The relation is linear for energies greater than 100 GeV, on the other hand, lower energies illustrate a bending initially from the cutoff energy $E_{\text{cut}} = 36.5$ GeV.

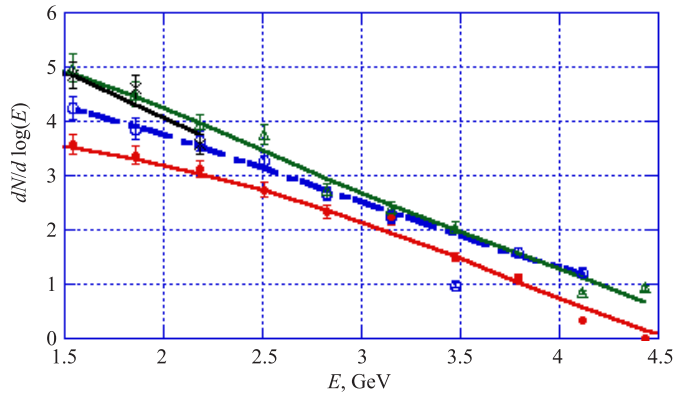

Fig. 7. The energy spectrum (in logarithmic scale) of muons penetrating the CMS cavern produced by primary photons. The four curves are corresponding to primary energies, from down to up, 10^{17}, 10^{18}, 10^{19} and 10^{20} eV, respectively

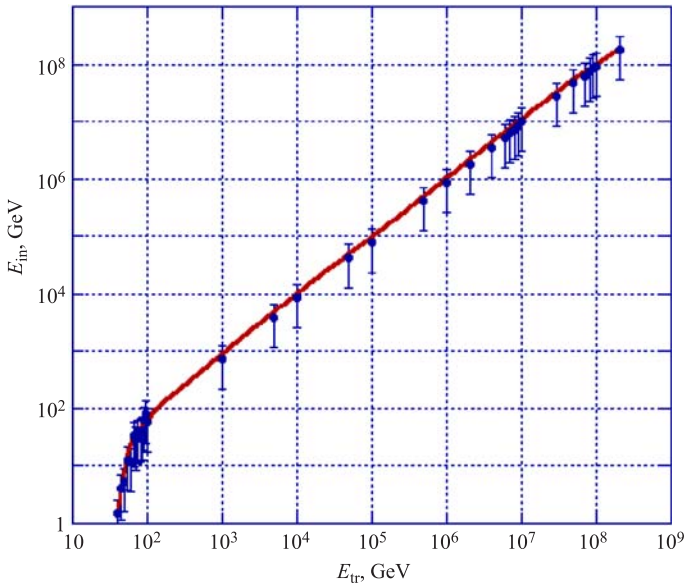

Fig. 8. The relationship between the energy of primary incident muons at ground level $E_{\rm in}$ and energy of transmitted muons to the CMS detectors $E_{\rm tr}$

4. SUMMARY AND CONCLUSIONS

We studied the propagation of energetic atmospheric muons produced by cosmic ray protons and photons, within the energy range 10^{17}–10^{20} eV, traveling through the soil above the CMS cavern. Our simulations prove that muons with energy less than 36.5 GeV could not be able to penetrate the cavern and will be completely absorbed in the soil. Such energetic muons could be produced by air showers with primary proton energy $> 10^{17}$ eV. The muons

produced by higher energies can penetrate the CMS cavern with energy spectrum shown in Figs. 6 and 7, which should be detected as a background in the tracking detectors of the CMS experiment.

The energy spectrum curves of muons reaching the ground level produced by primary protons demonstrate a variety in muon energy within the range $0.01–3.2 \cdot 10^5$ GeV, this energy range was $0.03–3.2 \cdot 10^4$ GeV in case of primary photons.

The lateral distribution of muons produced by primary protons and photons illustrates that muon component of the shower width is covering a circular area of radius 1.8 km from the shower core; in addition, the muon density produced by primary protons is ten times larger than that produced by primary photons.

Acknowledgements. We would like to thank the authorities at CERN for their help, especially the CMS team. We also thank Prof. J. Ellis for his helpful discussion and advice.

REFERENCES

1. *Mahrous A. et al.* Muon-Induced Air Showers Affecting CMS Tracking Detector // Proc. of the 29th Intern. Cosmic Ray Conf. India, 2005. P. 101–104.
2. *Hughes V., Wu C.* Muon Physics. Acad. Press, 1977. P. 1–9.
3. *Duldig M.* Muon Observations // Space Sci. Rev. 2000. V. 93. P. 189–208.
4. *Caso C. et al.* Review of Particle Physics // Eur. Phys. J. 2000. V. 3. P. 1–15.
5. *Andres E. et al.* Observation of High-Energy Neutrinos Using Cerenkov Detectors Embedded Deep in Antarctic Ice // Nature. 2001. V. 410. P. 441–443.
6. *Rossi B.* High-Energy Particles. Prentice-Hall, 1952.
7. *Groom N. et al.* Muon Stopping Power and Range Tables 10 MeV – 100 TeV // At. Data and Nucl. Data Tables. 2001. V. 78, No. 2. P. 183.
8. *Dawson R.* High-Energy Phenomenology // UNICAMP Campaigns, Brazil, July 13–17, 1998.
9. *Klein S. et al.* An Experimental Test of the LPM Effect: Bremsstrahlung Suppression at High Energies // Meeting of the Division of Particles and Fields of the Am. Phys. Soc., Batavia, 1992. P. 10–14.
10. *Polityko S. et al.* Muon's Behaviors under Bremsstrahlung with Both the LPM Effect and the Ter-Mikaelian Effect and Direct Pair Production with the LPM Effect // Nucl. Instr. Meth. B. 2001. V. 173. P. 30–36.

Received on June 23, 2008.